

# Nickel-Based Nanoporous Electrodes for Water Treatment

Elisa Sechi\*, Annalisa Vacca, Michele Mascia, Simonetta Palmas

Dipartimento di Ingegneria Meccanica, Chimica e dei Materiali, Università degli Studi di Cagliari, Piazza D'armi, 09123, Cagliari  
e.sechi@dimcm.unica.it

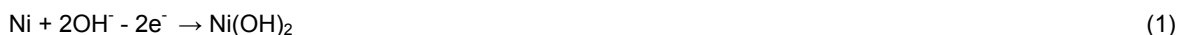
In this work nickel (Ni) nanoporous electrodes have been prepared by selective electrochemical dissolution of copper (Cu) from Ni-Cu deposits. The anodic dissolution of Cu was carried out in aqueous solutions containing boric acid (0.5M) using both constant voltage and pulsed voltage waveforms. Scanning electron microscopy (SEM), energy dispersive X-ray analysis (EDX) and Auger electron Spectroscopy (AES) showed that porous nickel foams with average size of 100-300 nm have been obtained under the operative conditions adopted. The electrodes have been characterized by cyclic voltammetry (CV) and linear sweep voltammetry (LSV) in alkaline solutions in order to investigate the electrocatalytic activity of porous nickel electrodes towards the oxygen evolution reaction (OER) and the removal of phenol, used as model of pollutant compounds.

The results demonstrated that nickel porous electrodes show electrocatalytic activity towards OER and are able to decrease the concentration of phenol in alkaline solutions.

## 1. Introduction

Metal oxides and their mixtures are widely used as catalysts and electrocatalysts in several processes; among the others, the oxygen evolution reaction deriving from the oxidation of water plays an important role in environmental applications. It is well known that electrochemical degradation of organic molecules at the so-called *active anodes* (i.e. IrO<sub>2</sub> or RuO<sub>2</sub>) takes place simultaneously with the oxygen evolution reaction which involves the formation of highly oxidised sites: at these sites the oxidation of organic reactants competes with oxygen evolution due to chemical decomposition of the oxides with higher oxidation state (Simond et al., 1997). Among the metals oxide, nickel based materials present different advantages such as commercial availability, low toxicity and good corrosive resistance in alkaline solutions. Moreover, nickel electrodes have been early proposed for the degradation of several organic compounds such as amines and alcohols (Fleischmann et al., 1971).

At nickel electrodes the commonly accepted mechanism for the formation of highly oxidation sites involves the hydroxylation of the nickel surface as follows: (Hutton et al., 2010):



where Ni(OH)<sub>2</sub> layer forms under open circuit potential in alkaline solutions. In recent studies (Medway et al., 2006; Juodkazis et al., 2008) it has been suggested that nickel is passivated by several molecular layers of nickel oxide NiO covered with a compact layer of Ni(OH)<sub>2</sub> hydroxide staying in contact with solution. At higher anodic potential Ni(II) shifts to Ni(III) following the reaction (Fleischmann et al., 1971) :



NiOOH sites react to form oxygen but they can also be exploited for the oxidation organic pollutant present in the solution.

In addition to the intrinsic electrocatalytic properties of the electrode materials deriving from their chemical nature, the electrochemical performances of the electrodes also depend on the geometric factors related to the extension of the surface area. Nanoporous structures of metals or metal oxides presenting high surface area can be obtained by selectively dissolving the more reactive metal component from an alloy system, often

with the aid of an electric field (Ding et al., 2004). Porous nickel foams can be produced by the selective dissolution of copper from Ni/Cu films: although nickel is more reactive than copper, the formation of a passive oxide film on nickel allows the dissolution of copper leading to a porous nickel foams. With this technique different nickel foams have been obtained: results have shown that the morphology of the porous structures depends on the composition of Cu/Ni film electrodeposited and on the electrochemical conditions for the selective corrosion (Zhang et al., 2014; Sun et al., 2004).

In this work the electrochemical behavior of porous nickel foams produced by the electrochemical anodic dissolution of Cu-Ni films has been studied. The electrodeposition of Cu-Ni films was carried out on boron doped diamond electrodes in aqueous solutions using a constant voltage. The selective anodic dissolution of copper has been performed in aqueous solutions, adopting constant and pulsed voltage conditions. The electrodes were characterized by cyclic voltammetry, before and after each electrochemical step. The morphology and the composition of the prepared electrodes have been analyzed by scanning electron microscopies and energy-dispersive X-ray spectroscopies. The electrocatalytic activities of porous nickel foams have been tested towards the oxygen evolution reaction (OER) and removal of phenol used as a model compound.

## 2. Experimental

### 2.1 Chemicals

Boric acid ( $\text{H}_3\text{BO}_3$ ) and potassium hydroxide (KOH) were purchased from Sigma-Aldrich®. Sodium sulphate anhydrous ( $\text{Na}_2\text{SO}_4$ ), nickel sulphate hexahydrate ( $\text{NiSO}_4 \cdot 6\text{H}_2\text{O}$ ), copper sulphate pentahydrate ( $\text{CuSO}_4 \cdot 5\text{H}_2\text{O}$ ), phenol ( $\text{C}_6\text{H}_6\text{O}$ ), glycerol ( $\text{HOCH}_2\text{CH}(\text{OH})\text{CH}_2\text{OH}$ ) and sulfuric acid ( $\text{H}_2\text{SO}_4$ ) were supplied by Carlo Erba.

### 2.2 Electrochemical Set-up

All electrochemical experiments were performed at room temperature using an AUTOLAB PGSTAT302N (Metrohm, Switzerland) potentiostat/galvanostat equipped with a frequency response analyser controlled with the NOVA software.

A classical three-electrode cell ( $V=10$  ml) was adopted, in which a Saturated Calomel Electrode (SCE) and a platinized titanium grid were used as reference and counter electrode, respectively. The working electrodes were inserted in a Teflon holder: the exposed geometrical area was  $0.5 \text{ cm}^2$ .

### 2.3 Electrochemical synthesis and characterization of porous nickel electrodes

Boron doped diamond (BDD) was used as inert material for the preparation of the nickel porous electrodes. Prior to electrochemical deposition, BDD was polished with water and acetone on a cloth polishing pad and then submitted to galvanostatic runs ( $0.1 \text{ mA}$ ) in  $0.5 \text{ M H}_2\text{SO}_4$  for 30 minutes. The electrodes were then rinsed with double-distilled water. The freshly BDD polished electrodes were subjected to electrodeposition in a plating solution containing  $0.5 \text{ M NiSO}_4$ ,  $0.005 \text{ M CuSO}_4$  and  $0.5 \text{ M H}_3\text{BO}_3$  ( $\text{pH}=4$ ), using a constant potential of  $-0.8 \text{ V}$  for a total time of 130 minutes and under gentle stirring conditions. The amount of charge passed during the electrodeposition was of  $4 \text{ C}$ .

The Ni-Cu films have been subjected to anodic dissolution in aqueous solutions, containing  $0.5 \text{ M H}_3\text{BO}_3$  and  $0.5 \text{ M Na}_2\text{SO}_4$  ( $\text{pH}= 3.8$ ). The experiments were carried out at pulsed voltage modulated between  $V_1$  ( $0.5 \text{ V}$ ) and  $V_2$  ( $0.07 \text{ V}$ ) for time durations of  $t_1$  ( $1 \text{ s}$ ) and  $t_2$  ( $5 \text{ s}$ ), respectively, for a total time of 30 minutes. Stirring conditions were also used during this electrochemical step. For comparison, the anodic dissolutions have also been performed at a constant voltage of  $0.5 \text{ V}$  for 30 minutes. For clarity, in the rest of the text we are going to call the samples produced using constant and pulsed voltage as “Const-Ni-foams” and “Pulse-Ni-foams”, respectively.

The electrodes have been characterized after each electrochemical step by cyclic voltammetry at scan rate of  $100 \text{ mV/s}$  in  $0.5 \text{ M Na}_2\text{SO}_4$  solutions; the potential was varied from the open circuit potential (OCP) to  $1 \text{ V}$  vs. SCE and back to  $-0.8 \text{ V}$  vs. SCE. The total capacitance of the electrodes was calculated from CV using the attained current density at  $0.25 \text{ V}$ . Finally, the electrodes at which the highest total capacitance was obtained, have been investigated about their electrocatalytic activity, towards OER and phenol removal. Prior to test the electrocatalytic activities, the electrodes were conditioned by potential cycling, over 150 times, between  $0$  and  $0.8 \text{ V}$  vs SCE at  $50 \text{ mV/s}$  in  $1 \text{ M}$  of KOH. The kinetic parameters of the OER process were determined by linear sweep voltammetry (LSV) in the potential range from  $E= 0.2$  and  $0.65 \text{ V}$  at sweep rate of  $0.5 \text{ mV/s}$  in  $1 \text{ M}$  KOH. To obtain overpotential  $\eta$  values, reversible oxygen potential was taken as  $250 \text{ mV}$  vs SCE (Corrigan DA et al., 1989). The anodic oxidation of phenol was firstly evaluated by cyclic voltammetry in  $0.1 \text{ M}$  KOH containing  $28 \text{ ppm}$  of phenol, followed by degradation experiments. These were carried out both in potentiostatic and galvanostatic mode at  $1 \text{ V}$  and  $5 \text{ mA}$  respectively, using solutions containing  $14 \text{ ppm}$  of phenol. During the runs, samples of electrolyte were withdrawn and analyzed for the concentration of reactant by 4-

aminoantipyrine method (ASTM 5530D) using UV spectrophotometer (Agilent Technologies, Cary Series Spectrophotometer).

A scanning electron microscope (SEM) equipped with EDX detector (Zeiss, Germany) was used to characterize the morphology and the chemical composition of the electrodes after and before the anodic dissolution. Auger electron Spectroscopy (AES) was also used to investigate the distribution of the elements constituting the Ni/Cu deposits.

### 3. Results and discussion

Figure 1-a displays the SEM images of the electrodeposits obtained at -0.8V. It can be appreciated a regular and homogeneous distribution of the deposits on the BDD surface. This kind of electrodeposition was further studied using Auger electron spectroscopy. The Auger mappings of Ni and Cu, illustrated in Figure 1-b and 1-c, respectively confirm a uniform composition of the deposits and reveal a homogeneous distribution of each element on the substrate. The EDX analysis of the Ni-Cu films shows a molar fraction of 0.4 and 0.58 for nickel and copper, respectively. This means that a deposition potential of -0.8 V allows the electrodeposition of both elements on the BDD surface in a similar content. Previous reports have shown that to prepare a better porous structure the component being etched should generally be near or higher than 50% (Chang at al.,2007).

The voltammogram measurements of the Ni-Cu deposits represented in Figure 2 show a single anodic peak at about 0.3 V associated to the stripping of the deposited copper on the BDD surface. On the reverse scan a cathodic peak is seen at -0.4 V due to the reduction of copper. The reduction-oxidation peaks related to nickel behaviour cannot be observed because of the formation of a passive oxide film on its surface (Sun et al., 2004).

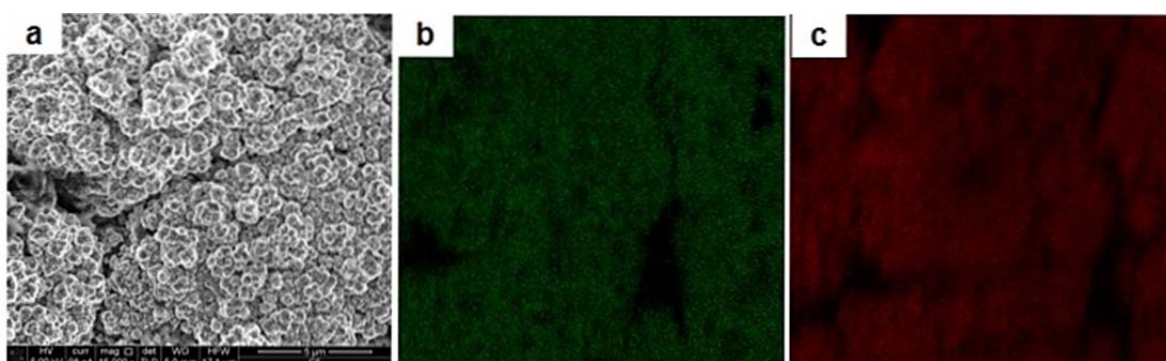


Figure 1: SEM image of Cu-Ni deposits (a) obtained at -0.8, Auger mappings of nickel (b) and copper (c) of the deposits

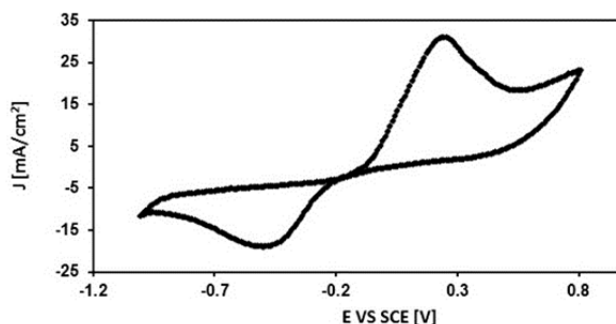


Figure 2: CV response of Ni-Cu deposits recorded in 0.5 M  $\text{Na}_2\text{SO}_4$  at scan rate of  $100 \text{ mV s}^{-1}$ .

The pulse bias was set slightly above to the OCP value in order to guarantee a generation of a very low current.

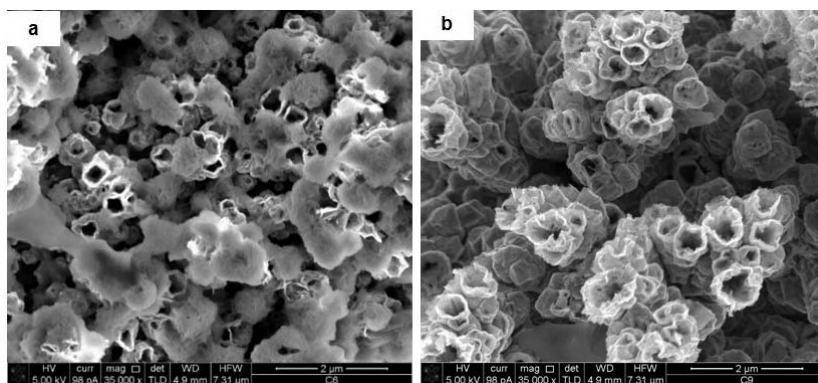


Figure 3: SEM image of the Const-Ni-foams (a) and Pulse-Ni-foams (b)

Earlier studies report that minimum current flow is necessary for the relaxation steps in order to avoid the re-deposition or dissolution of Cu, giving the time to atoms to reorganize without disturbance (Erlebacher et al., 2001).

Figure 3 displays the SEM images related to the anodic dissolution results for the two experimental conditions. It can be observed that a porous structure was achieved with different characteristics, which depended on the operative conditions. Moreover, in opposite to Const-Ni-foams, Pulse-Ni-foams present an almost total absence of copper deposits on their surface, occurrence also confirmed by EDX analysis (table-1). Anyway, both the electrodes display pores sizes in the range of 100-300 nm and the presence of oxygen on their surface. In addition, it is evident that a higher porosity and a homogeneous pores distribution has been obtained using pulsed voltage conditions.

Table 1: Composition and sizes of the Ni porous electrodes obtained from EDX and SEM analysis.

Sample	X <sub>Cu</sub> (%)	X <sub>Ni</sub> (%)	X <sub>O</sub> (%)	d(nm)
Const-Ni-foams	48	28	23	100-300
Pulse-Ni-foams	-	92	6	100-300

Capacitive measurements have been performed in order to determine the total capacitance  $C_t$  of the electrodes that represents a measure of the real surface area (Berenguer et al., 2009).

The capacitance was calculated from CV (data not shown) using the attained current density  $J$  at 0.25 V (scan rate  $v = 100$  mV/s), by the following equation:

$$C_t = J/v \quad (3)$$

In this equation  $I$  is equal to  $(J_a - J_c) / 2$ , where  $J_a$  and  $J_c$  are the anodic and cathodic current density, respectively.

The obtained values of the total capacitance were of 2600 and 5100  $\mu\text{F}/\text{cm}^2$  for the Const-Ni-foams and Pulse-Ni-foams, respectively. These results are in agreement with SEM analysis, discussed above.

Since Pulse-Ni-foams exhibited a greater capacitance value and porosity, which are determining factors for the electrocatalytic activity, these samples have been studied for OER and phenol oxidation.

Figure 4 displays the cyclic voltammograms recorded over 150 times between  $V = 0$  mV and 800mV at scan rate of 50mV/s in 1 M KOH. It can be appreciated the anodic and cathodic peak associated to the transition Ni(II)/Ni(III) at 0.1 V and 0.45 V, respectively. It worth to be noticed that the current peaks increase remarkably with the number of scans. This can be attributed to an enrichment of the Ni(III) species at the surface of the electrode with increasing of the scans, resulting in a thicker electrocatalytic layer (Yuqing et al., 2013)

The Figure 5 shows the polarization curve of the electrodes in 1M KOH. The kinetic parameters were determined from the linear part of the tafel plot, which provides information about the mechanism (slope  $b$ ) and rate (exchange current density  $j_0$ ) of OER. It can be observed the presence of two well-defined Tafel regions at low (100-200 mV) and high overpotential (200-400mV), respectively. This behaviour is probably caused to the change in the valence state of the active sites of the catalyst and by influence of higher oxide on OER (Da Silva et al., 1997; Corrigan et al., 1989).

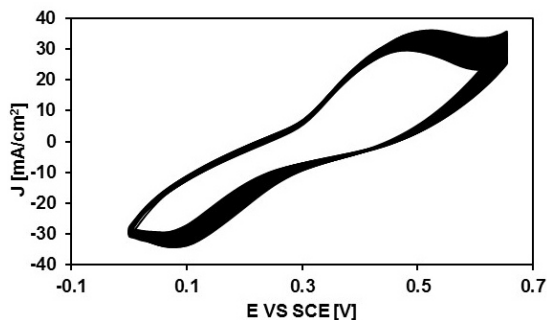


Figure 4: Cyclic voltammogram of the Pulse-Ni-foams in 1 M KOH at scan rate of  $50 \text{ mV s}^{-1}$

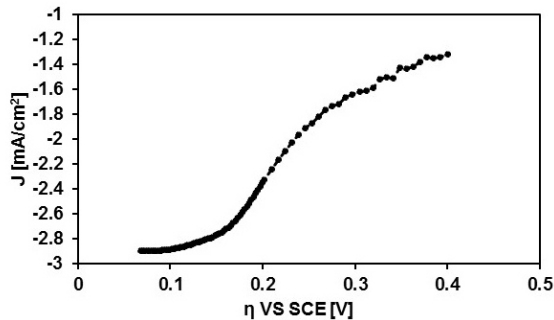


Figure 5: Tafel plot for OER of the Pulse-Ni-foams in KOH 1 M at sweep rate of  $0.5 \text{ mV s}^{-1}$ .

An analogous behaviour was reported for smooth nickel electrodes in alkaline media (Kibria and Tarafdar, 2002). The obtained  $b$  values for high  $\eta$  and low  $\eta$  are comparable than those of smooth Ni electrodes (G Lyons et al., 2008; Kibria and Mridha, 1996). Regarding the  $j_0$  values of 0.2 and  $0.003 \text{ mA/cm}^2$  were obtained for high and low overpotential, respectively. Compared to a smooth nickel anode the obtained  $j_0$  value for low  $\eta$  region was six order of magnitude higher; whereas for high  $\eta$  region was about 2 order of magnitude higher (Kubisztal and Budniok, 2008); The remarkable increase can be attributed to the enhanced surface area of the porous electrodes.

The Figure 6 displays the cyclic voltammetry of the porous nickel electrode in 0.1 M KOH solution with or without 28 ppm of phenol. As can be seen upon the addition of phenol both the anodic and cathodic peak currents slightly enhanced, indicating that phenol can react with NiOOH sites electrochemically formed, as proposed in (Fleishmann et al, 1971), where the electrochemical oxidation of many organic compounds with Ni anodes in alkaline electrolyte is mediated by NiOOH and can be sketched as follows:



As for the OER a greater surface area due to the porosity of the electrode allows generating a great number of active sites for the formation Ni (II)/Ni (III) redox couples.

Figure 7 shows that the degradation process of phenol can be achieved both under galvanostatic and potentiostatic conditions. Moreover, it can be noticed that the process follows a pseudo-first-order kinetics and the degradation rate is not affected by current density, under the operative conditions adopted in this work, indicating a mass transfer controlled process.

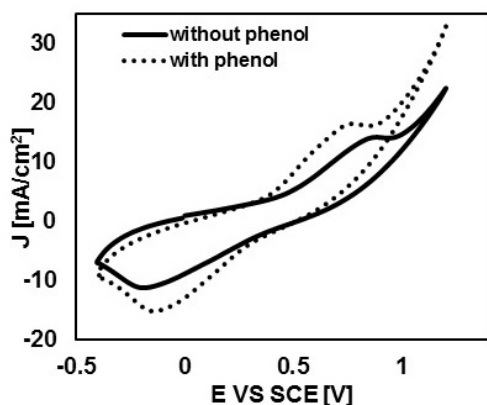


Figure 6: CV of Pulse-Ni-foams in the presence or absence of 28 ppm of phenol in 0.1M KOH

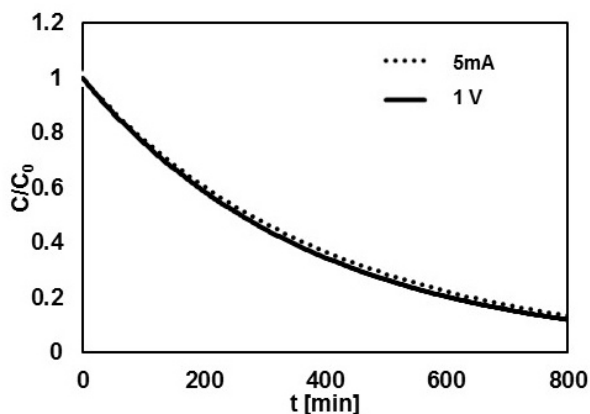


Figure 7: Trend of phenol concentration during oxidation at 1V and 5mA in 0.1M KOH by Pulse-Ni-foams

#### 4. Conclusions

The results presented in this work indicate that nanoporous nickel electrodes synthesized by selective anodic etching of copper from Ni-Cu deposits, can be effectively employed as anodes for degradation of organic compounds and for OER in alkaline solutions.

Depending on the conditions adopted for the etching, different surface areas were obtained, the highest being those obtained under pulsed potential.

Moreover, the results show that the high surface areas allow obtaining values of exchange currents for OER from two to six order of magnitude higher than smooth Ni electrodes.

Finally, the electrodes were tested for organic removal from water, using phenol as model compound: the removal of phenol was achieved under all the conditions adopted. The degradation occurs in the region of oxygen evolution, confirming that the oxidation is mediated by surface oxides electrogenerated. The kinetics was very fast, being the mass transfer the controlling step.

## Reference

- Berenguer R., Quijada C., Morallón E., 2009, Electrochemical characterization of SnO<sub>2</sub> electrodes doped with Ru and Pt, *Electrochimica Acta* 54, 5230-5238
- Chang JK., Hsu Sh., Sun IW., Tsai WT., 2008, Formation of Nanoporous Nickel by Selective Anodic Etching of the Nobler Copper Component from Electrodeposited Nickel-Copper Alloys, *J. Phys. Chem. C*, 112, 1371-1376
- Comninellis C., De Battisti A., 1996, Electrocatalysis in anodic oxidation of organics with simultaneous oxygen evolution, *Journal de Chimie Physique et de Physico-Chimie Biologique* 93, 673-679
- Corrigan DA, Bendert R.M., 1989, Effect of coprecipitated metal ions on the electrochemistry of nickel hydroxide thin films: cyclic voltammetry in 1 M KOH, *J Electrochem Soc* 136,723-728.
- Da Silva LA., Alves V.A., Trasatti S., 1992, Surface and electrocatalytic properties of ternary oxides iro.3TI(0.7-X)PtXO<sub>2</sub>, Oxygen evolution from acidic solution, *J Electroanal Chem* 427, 97-104
- Ding Y., Kim Y.J., Erlebacher J., 2004, Nanoporous Gold Leaf: "Ancient Technology", *Advanced Material*, *Advanced Materials* 16, 1897-1900
- Erlebacher J., Aziz MJ., Karma A., Dimitrov N., Sieradzki K., 2001, Evolution of nanoporosity in dealloying, *Nature* 410, 450-453
- Fleischmann M., Korinek K., Pletcher D., 1971, The oxidation of hydrazine at a nickel anode in alkaline solution, *J. Electroanal. Chem* 34, 499-503
- Hutton LA., Vidotti M., Patel AN., Newton ME., Unwin P.R., Macpherson J.V., 2010, Electrodeposition of Nickel Hydroxide Nanoparticles on Boron-Doped Diamond Electrodes for Oxidative Electrocatalysis, *J. Phys. Chem. C* 115, 1649-1858
- Juodkazis K., Juodkazytė J., Vilkauskaitė R., Jasulaitienė V., 2008, Nickel surface anodic oxidation and electrocatalysis of oxygen evolution, *J Solid State Electrochem* 12, 1469-1479
- Kibria AKMF., Tarafdar SA., 2002, Electrochemical studies of a nickel copper electrode for the oxygen evolution reaction, *International Journal of Hydrogen Energy* 27, 879-884
- Kibria M.F., Mridha M. SH., 1996, Electrochemical studies of the nickel electrode for the oxygen evolution reaction, *Int. J. Hydrogen Energy* 21,179-182,
- Kubisztal J., Budniok A., 2008, Study of the oxygen evolution reaction on nickel-nased composite coatings in alkaline media, *International J. of hydrogen Energy* 33, 4488-4494
- Lyons M.E.G., Brandon M.P., 2008, The Oxygen Evolution Reaction on Passive Oxide Covered Transition Metal Electrodes in Aqueous Alkaline Solution, *Int. J. Electrochem. Sci* 3, 1386 - 1424
- Medway S.L., Lucas C.A., Kowal A., Nichols R.J., Johnson D., 2006, In situ studies of the oxidation of nickel electrodes in alkaline solution, *J Electroanal Chem* 587, 172 - 181.
- Miao Y., Ouyang L., Zhou S., Xu L., Yang Z., Xiao M., Ouyang R., 2014, Electrocatalysis and electroanalysis of nickel, its oxides, hydroxides and oxyhydroxides toward small molecules, *Biosensors and Bioelectronics* 53, 428-439
- Simond O., Schaller V., Comninellis C., 1997, Theoretical model for the anodic oxidation of organics on metal oxide electrodes, *Electrochim. Acta* 42, 2009-2012
- Sun L., Chien CL., Searson P.C., 2004, Fabrication of Nanoporous Nickel by Electrochemical Dealloying, *Chem. Mater* 16, 3125-3129.
- Zhang J., Zhan ., Bian H., Li Z., Tsang CK., Lee C., Cheng H., Shu S., Yang Yang L., Lu J., 2014, Electrochemical dealloying using pulsed voltage waveforms and its application for supercapacitor electrodes, *Journal of Power Sources* 257, 374-379.